**GACP ACCOMPLISHMENT REPORT**

James A. Coakley, Jr.

College of Oceanic and Atmospheric Sciences
Oregon State University
Corvallis, OR 97331-5503

**Title:** Limits to Cloud Susceptibility

## Tasks Completed, Year 2

Tasks completed during the second year were as follows: 1) Development was completed on the algorithms used to identify 1-km AVHRR and 2-km VIRS fields of view that were overcast by optically thick ($\tau > 2$) clouds that were part of single-layered cloud systems. 2) A scheme was developed for retrieving optical depth, effective droplet radius, and cloud emission temperature from AVHRR and VIRS data. 3) 680 ship tracks in NOAA-14 and 395 ship tracks in NOAA-12 AVHRR observations of the U.S. West Coast for June 1999 were located and logged (by hand). These ship tracks were in addition to the 337 in NOAA-11 and 421 in NOAA-12 observations for the June 1994 MAST period logged last year. 4) A scheme was developed that combined the positions of the tracks logged by hand with rudimentary pattern recognition techniques to automatically identify the pixels that made up a ship track and separate the contaminated pixels from the surrounding uncontaminated pixels. 5) Because the intent is to compare polluted clouds with clouds that are in every way similar except for the pollution, autocorrelations of retrieved optical depths, droplet radii, and cloud emission temperatures were obtained for observations of extensive stratus decks. The autocorrelation lengths derived from the correlations indicate the size of the domain from which clouds with similar properties can be extracted. 6) The scene identification, cloud retrieval, and ship track identification schemes were applied to all of the NOAA-14 and most of the NOAA-12 data for June 1999. In order to test the sensitivity of the findings to the size of the domain from which the properties of nearby unpolluted clouds were drawn for comparison with those derived for the ship tracks, results have been obtained using various sizes of the control domain. 7) While not part of the work originally proposed, W.R. Tahnk (supported by NSF through the Center for Clouds, Chemistry, and Climate, $C^4$) applied the scene identification and aerosol retrieval scheme employed in INDOEX to global NOAA-9 AVHRR data for June 1991. The results of the retrievals were summarized and submitted to GACP for comparison with the results of other retrieval schemes.

## Results

Analysis of the ship tracks in the NOAA-14 AVHRR observations for the U.S. west coast in July 1999 indicate that clouds contaminated by ships have smaller reflectivities at visible wavelengths than would be expected had the decreases in droplet radii been compensated by increases in droplet numbers so that cloud liquid water remained constant. The analysis of a ship track is illustrated in Figure 1. The figure shows a portion of a NOAA-14 image created from

3.7-μm radiances. In the image, pixels that are overcast by clouds contaminated by the ship, as identified by the automated routines discussed in the previous section, are rendered in color according to the retrieved droplet radii. Values of the mode radii are shown. For the droplet size distributions on which the retrievals are based, the effective radii are a factor of 1.55 times the mode radii. Not all track pixels are identified by the automated routines. The current algorithm does not allow for complex structures in the tracks, such as the intersection of two or more tracks. Such complexity in the track patterns leads to the rejection of track pixels in the current scheme. Nevertheless, as shown in the figure, the automated routine isolates many genuine track pixels and thus allows the separation of the contaminated pixels from nearby, uncontaminated pixels. The borders in the image outline the 30-km domain on either side of the tracks from which the properties of the uncontaminated clouds are obtained for comparison with those of the clouds contaminated by the ship. The borders are drawn on the basis of the location of the track as logged by hand.

Comparison of the contaminated and uncontaminated clouds along the track was performed for each 50-km segment along the track. Figure 2 shows results of such a comparison for one of the 50-km segments of the track shown in Fig. 1. Points in the figure represent pixel-scale values of the visible optical depth, droplet radius, and cloud emission temperature for the pixels identified as being contaminated within the 50-km segment and an equal number of pixels drawn randomly from the surrounding uncontaminated clouds. The results illustrate the difficulty in detecting the indirect radiative forcing due to aerosols. Changes in droplet radii are clearly significant. The error bars in the figure indicate the $\pm$ 2-$\sigma$ range about the mean. The changes in droplet radius, however, are a consequence of the selection criteria used to identify the track pixels. The visible optical depth shows little change (~ 3), compared with the pixel to pixel variability in optical depth ($\pm$ 8). If cloud liquid water were to remain constant, then the fractional change in the visible optical depth would be related to the fractional change in the droplet radius by

$$\frac{\Delta\tau}{\tau} = -\frac{\Delta r}{r}. \qquad (1)$$

Based on the fractional change in droplet radius, the optical depth should have increased by ~ 3 for the pixels identified as containing the ship track, as it appears to have done. The change in emission temperature is small compared with the natural variability exhibited by the overcast pixels.

Figure 3 summarizes results for over 450 50-km track segments drawn from the July 1999 NOAA-14 observations. Autocorrelation lengths for visible optical depths, droplet radii, and cloud emission temperatures derived from observations of extensive stratus decks were typically shorter than 20 km. As a result, each 50-km segment can be taken as an independent estimate of the fractional changes in optical depth and droplet radius. The diagonal line in Fig. 3 is given by (1). The line divides the optical depth-droplet radius domain into regions for which 1) the indirect effect by aerosols appears to be enhanced, as would be the case if the polluted clouds had more liquid water than the surrounding unpolluted clouds; 2) a region for which the effect is reduced, as would be the case were the polluted clouds to have less liquied water or were the aerosol to significantly increase the absorption of sunlight by the clouds; and 3) a region for which the unpolluted clouds have higher reflectivities than the polluted clouds. The spread of the results illustrates the effect of the large natural variability in cloud liquid water, even for scales of 1 km. Despite the large natural variability exhibited by clouds, the results indicate that polluted clouds generally have higher reflectivities than their unpolluted counterparts, but that the increase in reflectivities is less than would be expected if cloud liquid water and the amount of sunlight absorbed by clouds were to remain constant.

**Statement of Work, Year 3**

During the first two years, algorithms were developed to 1) identify fields of view in imagery data that were overcast by low-level stratus and to distinguish these fields of view from those that were only partially cloud covered; 2) retrieve optical depths, effective droplet radii, and cloud emission temperatures for the overcast pixels, and 3) automatically identify pixels containing ship tracks and distinguishing these pixels from surrounding pixels overcast by uncontaminated clouds. In addition, over 1800 ship tracks have been identified and their positions logged for NOAA-11, 12, and 14 passes of June 1994 and July 1999 over the U.S. west coast. Of these, all of the ship tracks for the July 1999 NOAA-14 and most of the tracks for the July 1999 NOAA-12 passes have been analyzed. Preliminary results indicate that using Twomey's proposal of increasing droplet number and decreasing droplet radius so that cloud liquid water remains constant, leads to an aerosol indirect radiative forcing that is larger than observed, even for the marine stratus off the west coast, which is thought to be highly sensitive to modification by aerosols.

In view of the tasks accomplished, work for the third year is planned as follows: 1) complete the analysis of all tracks logged for the NOAA-11, 12, and 14 observations and prepare papers for publication that present the scene identification scheme, the cloud retrieval algorithm, and the findings of the ship track analyses. 2) Using the results for the analyzed tracks, assess the feasibility of pursuing the sensitivity of the findings to sun-target-satellite viewing geometry and to the distance along the track from the location of the ship. The distance from the ship is an indication of the time that the cloud has had to respond to the pollution. 3) A special pattern recognition scheme will be developed to analyze regions in which ship tracks intersect each other. Results for intersections should provide an assessment of the degree to which the indirect effect becomes saturated in polluted clouds. Papers presenting results will be prepared should the sensitivity studies noted above prove feasible and the analysis of track intersections is successfully undertaken. The AVHRR radiances used in the analysis along with the results of the scene identification, the cloud properties retrieved for pixels overcast by layered clouds, and the ship track pattern recognition scheme, will be prepared for the designated GACP archive.

Time permitting, ship track observations for the U.S. west coast will be sought in VIRS and MODIS data. These instruments obtain radiances at near infrared wavelengths (1.6 and 2.3 μm) suitable for determining cloud droplet effective radius. Such observations can be used to assess the sensitivity of the findings obtained with the AVHRR to the wavelengths of the reflected sunlight used to determine droplet radii. In addition, because the TRMM orbit precesses, the VIRS observations provide a range of sun-target-satellite viewing geometries not available to the AVHRR and MODIS observations. The wider range will provide further assessment of any sensitivity in the findings to viewing geometry.

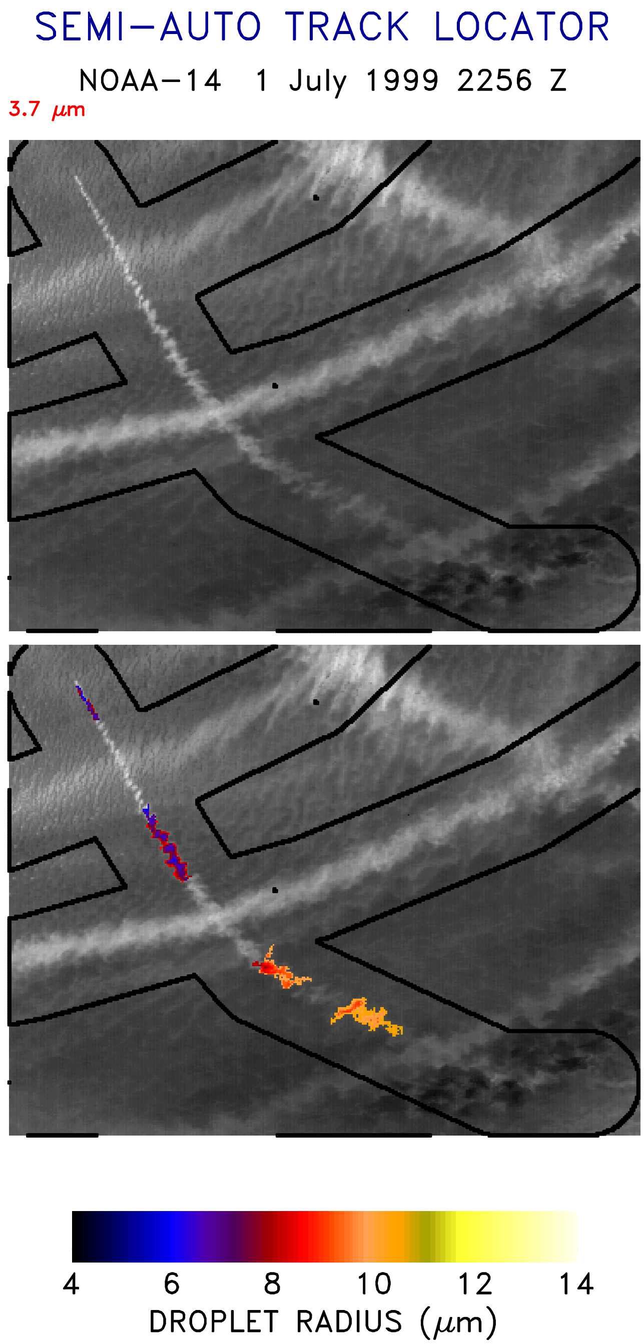


Figure 1. Example of results from automated track identification algorithm. 1-km AVHRR pixels identified as being overcast and contaminated by a ship track are rendered in color according to the retrieved value for the droplet radius. The black borders in the figure show the limits of the domains from which observations of surrounding, uncontaminated clouds are drawn for comparison with the clouds contaminated by ships.

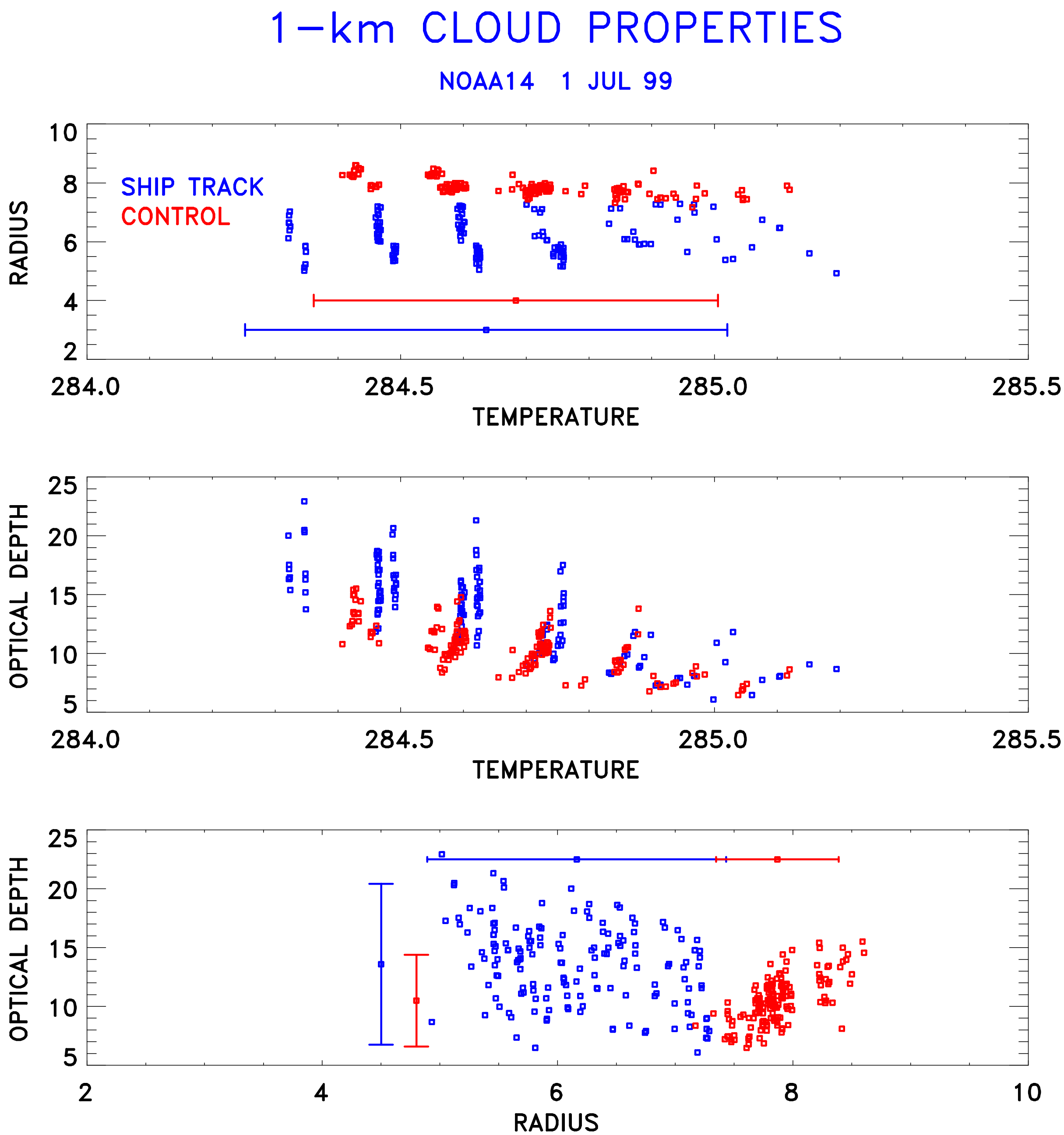


Figure 2. Droplet radii, visible optical depths, and cloud emission temperatures for pixels overcast by clouds identified as being contaminated by a ship and nearby pixels overcast by uncontaminated clouds. Error bars indicate the ± 2 σ range about the mean.

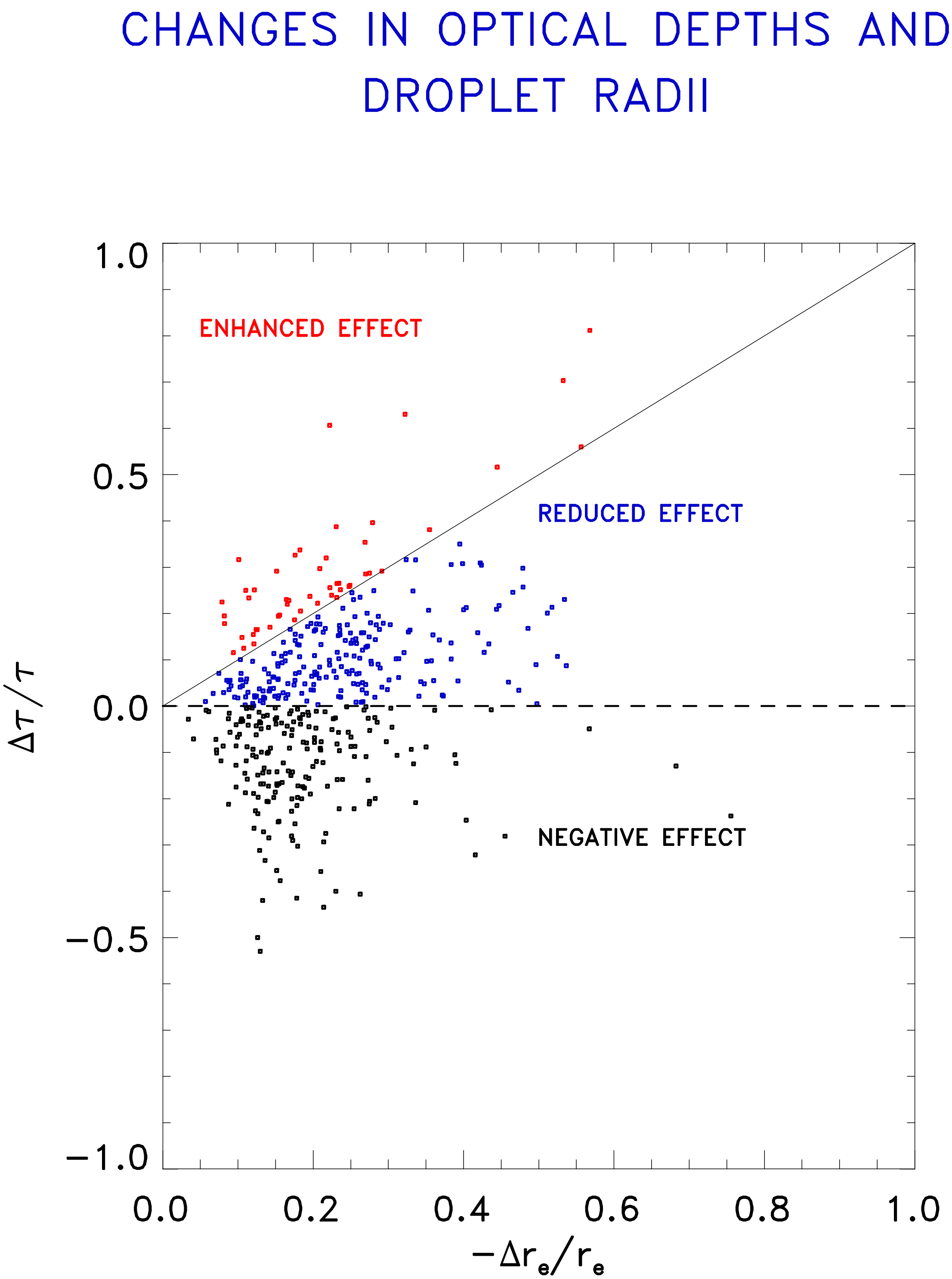


Figure 3. Summary of fractional changes in average optical depth and effective droplet radius for over 450 ship track segments obtained from the July 1999 overpasses of NOAA-14.